

## ON BOILING INCIPIENCE DUE TO CONTACT ANGLE HYSTERESIS\*

KEITH CORNWELL

Department of Mechanical Engineering, Heriot-Watt University,  
 Edinburgh, U.K.

(Received 18 March 1981 and in revised form 17 June 1981)

**Abstract**—The incipience of boiling on a metal surface is largely due to instability of the vapour-liquid interfaces which exist in minute natural cavities. The influences of surface roughness and contact angle on the equilibrium of the interface are studied and expressions relating roughness and advancing and retarding contact angles to the possibility of vapour trapping are developed.

A model of boiling incipience based on contact angle hysteresis between the advancing and retarding angles of the interface within the cavity is presented. This hysteresis arises naturally from the roughness and heterogeneity of a surface on the microscopic scale and thus occurs on normal engineering boiling surfaces. The model predicts incipience at smaller radii than the cavity mouth radii and successfully explains the observed features of boiling incipience without postulating the existence of re-entrant cavities.

### NOMENCLATURE

$A$ ,	surface area;
$\Delta G$ ,	Gibbs free energy change;
$h_{fg}$ ,	enthalpy of vaporisation;
$p$ ,	pressure;
$R$ ,	radius of spherical interface;
$R_e$ ,	radius of interface at equilibrium;
$s$ ,	surface roughness area ratio;
$T$ ,	temperature;
$\Delta T_{sat}$ ,	temperature difference between surface (or gas in cavity) and bulk liquid saturation;
$V$ ,	volume of gas and vapour in cavity;

$l$ ,	liquid;
$s$ ,	solid or surface;
$sat$ ,	saturation;
$v$ ,	vapour.

### 1. INTRODUCTION

THIS PAPER is about the surface factors that determine the commencement of boiling under normal conditions as encountered in engineering systems. It is concerned with the equilibrium of small amounts of gas and vapour trapped in cavities on surfaces and the conditions which allow growth to form bubbles. Knowledge of these conditions is important because the value of the heat transfer coefficient in the lower part of the nucleate boiling range is indirectly determined by them.

Boiling sites on normal metal surfaces are typically large enough to be examined under an electron microscope, but too small to be located by a surface probe. In an earlier study (Cornwell [1]) most of the first 50 sites to nucleate in water on a copper surface were located in order of incipience and examined. The site radii were typically around one micrometre and therefore approx. 10,000 times the lattice constant and 100 to 1000 times the oxide layer thickness (Fig. 1). The normal equations relating interfacial tensions are applicable down to an equilibrium radius of around  $0.01 \mu\text{m}$  (Woon *et al.* [2]) and may therefore be used in boiling site studies.

Contact angle variation has been advocated as the cause in incipience in liquid metals by Chen [3], and Holland and Winterton [4]. The model used in these papers involves meniscus flip-over within the cavity owing to surface material changes or reduction of the oxide layer by the liquid metal. Winterton [5] extended the model to a wider range of liquids by considering flip-over due to contact angle hysteresis and showed qualitatively the importance of advancing and retarding angles in trapping and incipience. The

### Greek symbols

$\beta$ ,	cavity half-apex angle (Fig. 2);
$\theta$ ,	contact angle (in degrees);
$\theta_a$ ,	maximum true advancing contact angle;
$\theta_m$ ,	apparent or mean contact angle;
$\theta_{mc}$ ,	apparent or mean contact angle at critical value for trapping (eqn. 9);
$\theta_r$ ,	minimum true retarding contact angle;
$\theta_t$ ,	true contact angle;
$\theta_{tc}$ ,	true contact angle at critical value for trapping (eqn. 12);
$\Delta\theta_{tc}$ ,	$\theta_{tc} - \theta_t$ (eqn. 13);
$\Pi^0$ ,	absorbed film vapour pressure;
$\rho$ ,	density;
$\sigma$ ,	surface free energy ( $\text{J/m}^2$ ) or surface tension ( $\text{N/m}$ );
$\phi$ ,	surface roughness angle (Fig. 5).

### Subscripts

$e$ ,	equilibrium;
$g$ ,	gas;

\* Paper written while on leave at the University of Iceland, Reyjavik.

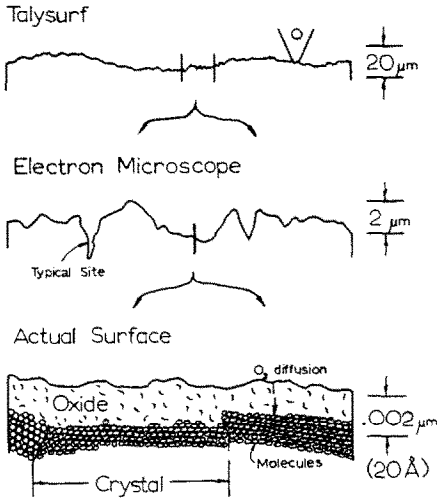


FIG. 1. Successive magnification of a typical machined surface. (Length scale as vertical scale.)

expression of contact angle hysteresis in terms of surface effects could not have been applied with any confidence to the cavity without the analysis and experimental vindication of a somewhat similar approach to plane surfaces by Johnson and Dette [6, 7]. The work described in this paper is essentially a theoretical examination of the mechanism of contact angle hysteresis and its effect on trapping and incipience.

2. THE EQUILIBRIUM INTERFACE RADIUS IN A CONICAL CAVITY

The equilibrium pressure difference across the interface between a liquid, and a gas and vapour mixture situated in a small conical cavity as shown in Fig. 2 is given by

$$p_g + p_v - p_l = \frac{2\sigma}{R_c} \quad (1)$$

The equilibrium radius  $R_c$  of the spherical interface may be positive or negative.

The interface is stable if a disturbance  $dp$  in the pressure difference across it leads to a change in  $2\sigma/R$  of similar sign.

$$\frac{d}{dp} \left( \frac{2\sigma}{R} \right) > 0.$$

Since a pressure disturbance of the gas-vapour mixture in the cavity causes a volume change  $dV$  of similar sign and  $\sigma$  is constant, the stability criterion may be expressed as

$$\frac{d}{dV} \left( \frac{1}{R} \right) > 0. \quad (2)$$

A small change of volume from 1 to 2 as shown in Fig. 3 may lead to an increase or decrease in  $R$  depending upon whether the contact angle remains constant or changes about the line of contact and the interface is convex or concave. Application of the stability criterion shows that the only unstable situation occurs in

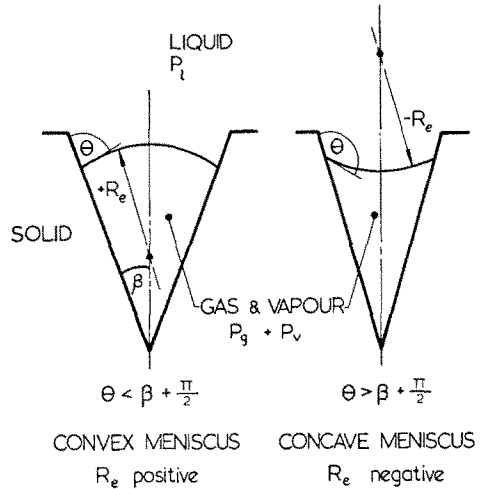


FIG. 2. The interface in a conical cavity.

case (b); in the other cases it is theoretically possible to trap the gas-vapour mixture. In practice the contact angle variation is limited and a reduction in gas pressure, say in case (a), may lead to movement as in case (b) and hence instability and flooding. When the line of contact is at the mouth, movement as in case (b) is geometrically impossible.

In boiling ( $p_v - p_l$ ) is generally small and may be related to the temperature difference  $\Delta T_{sat}$  between the gaseous phase or wall and the saturation temperature using the Clausius-Clapeyron equation to yield (at constant  $\sigma$ ),

$$\Delta T_{sat} = \frac{T_{sat}}{\rho_g h_{fg}} \left( \frac{2\sigma}{R_c} - p_g \right). \quad (3)$$

Incipience in a particular fluid-surface combination is therefore dependent upon  $R_c$  and  $p_g$ . Here we are concerned only with  $R_c$ , but the effect of non-condensable gas on the surface can be important in lowering the incipience superheat (see e.g. [8]).

3. CONTACT ANGLE HYSTERESIS DUE TO MICROSCOPIC ROUGHNESS AND SURFACE HETEROGENEITY

3.1. Introduction and definition of terms

The trapping, storage and expansion of minute

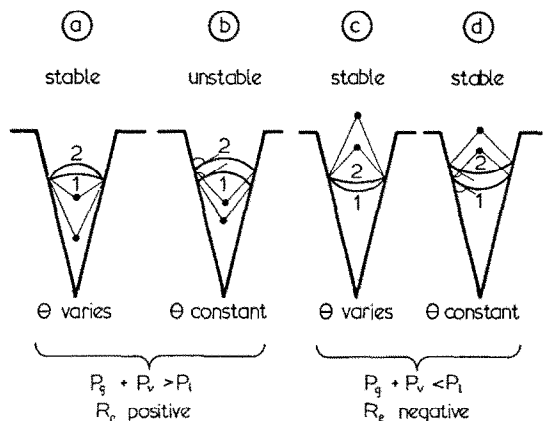


FIG. 3. Interface stability.

quantities of gas and vapour on a submerged surface requires the existence of a wide range of contact angles on the microscopic scale. In this section it is shown that normal metal surfaces exhibit this range of contact angles as a consequence of their basic geometry and surface chemistry.

Consider initially the conventional surface energy equations applied to a perfectly flat surface where the angle made by the liquid is the true contact angle  $\theta_t$ . This is often adequate for describing situations involving liquid drops and films on smooth surfaces where the liquid thickness is typically 1000 times the surface roughness. The surface free energy per unit area,  $\sigma$ , ( $J/m^2$ ) or surface tension ( $N/m$ ) between each phase may be represented as shown in Fig. 4(a). The change in free energy on displacing the liquid so that it covers and additional area  $\Delta A_s$  is given by

$$\Delta G_s = \sigma_{s1} \Delta A_s - \sigma_{sv} \Delta A_s + \sigma_{1v} \cos(\theta_t + \Delta\theta_t) \Delta A_s,$$

At equilibrium

$$\lim_{\Delta A_s \rightarrow 0} \left( \frac{\Delta G_s}{\Delta A_s} \right) = 0$$

and Young's equation is obtained

$$\sigma_{sv} - \sigma_{s1} = \sigma_{1v} \cos \theta_t, \quad (4)$$

In these equations it is assumed that the vapour is at the saturation vapour pressure. The term  $\sigma_{sv}$  therefore applies to the solid when coated with an adsorbed film of vapour and may be subdivided into the surface energy of the solid in a vacuum and the adsorbed film vapour pressure  $\Pi^0$

$$\sigma_{sv} = \sigma_s - \Pi^0. \quad (5)$$

In this paper the *surface* is considered hydrophilic or wetted by the liquid when  $0^\circ < \theta_t < 90^\circ$  and hydrophobic or unwetted when  $90^\circ < \theta_t < 180^\circ$ .

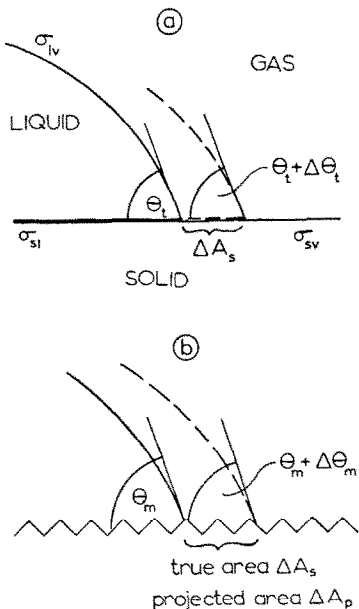


FIG. 4. The true and mean contact angles.

Consider now the microscopic contact angle very near the surface where the roughness cannot be ignored, as shown in Fig. 4(b). The change in free energy becomes

$$\Delta G_s = \sigma_{s1} \Delta A_s - \sigma_{sv} \Delta A_s + \sigma_{1v} \cos(\theta_m + \Delta\theta_m) \Delta A_p,$$

where  $\theta_m$  is the mean contact angle. If a surface roughness area ratio is defined as

$$s = \frac{\text{true area}}{\text{geometrical (or projected) area}} = \frac{\Delta A_s}{\Delta A_p},$$

then at equilibrium

$$\sigma_{sv} - \sigma_{s1} = \sigma_{1v} \frac{\cos \theta_m}{s}, \quad (6)$$

and from eqns. (4) and (6)

$$\cos \theta_m = s \cos \theta_t. \quad (7)$$

The parameter  $\theta_m$  is sometimes termed the apparent or measured contact angle, but it is strictly no more than a unique function of  $s$  and  $\theta_t$ , lying between the advancing and retarding angles. The measured angle is dependent on some average effect of these terms along the line of contact. In this work  $\theta_m$  is simply termed the mean contact angle. It is probably the nearest of the defined angles to the normal macroscopic contact angle often reported in the literature. Equation (6) is sometimes referred to as Wenzel's modification of Young's equation and a thermodynamic verification is given by Good [9]. Equation (7) indicates that for  $\theta_t < 90^\circ$ , roughness increases the equilibrium measured angle  $\theta_m$  and for  $\theta_t > 90^\circ$  roughness decreases it. (The correction for  $\theta_t = 60^\circ$  on a machined metal surface of  $a = 1.2$  is about  $5^\circ$ .)

### 3.2. The effect of cavity wall micro-roughness on the contact angle within the cavity

The nucleation site is idealized as a conical cavity with the roughness of the wall represented by a wedge-

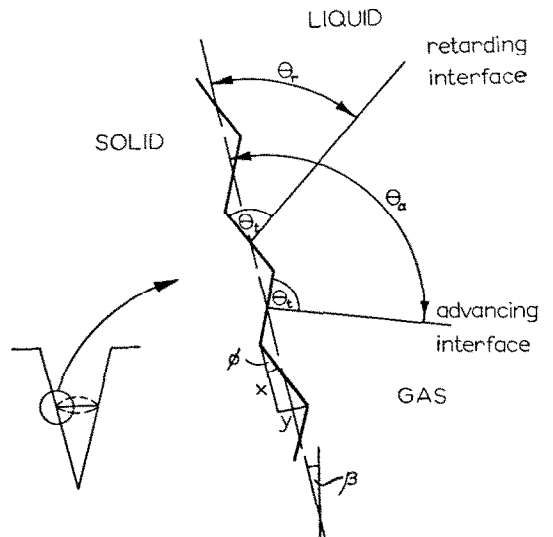


FIG. 5. Micro-roughness of the cavity wall.

shaped function forming grooves around the cavity shown in Fig. 5. For the moment  $\theta_i$  is assumed to be constant and the cavity is assumed to be a unique indentation on an otherwise horizontal surface and sufficiently larger than the surface asperities for the roughness concept [eqn. (7)] to be applied to the walls. The combination of eqn. (7) with the geometry of the arrangement shown in Fig. 5 yields the following set of equations:

$$\frac{1}{s} = \frac{x}{\sqrt{(x^2 + y^2)}} = \cos \phi \quad (8a)$$

$$\cos \theta_m = s \cos \theta_i \quad (8b)$$

$$\theta_a = \theta_i + \phi \quad (8c)$$

$$\theta_r = \theta_i - \phi \quad (8d)$$

Angles  $\theta_a$ ,  $\theta_r$ , and  $\theta_i$  are plotted as a function of  $s$  for three values of the mean angle  $\theta_m$  in Fig. 6. Thus, for example, at  $\theta_m = 60^\circ$  on a surface of area ratio 1.2, the values of  $\theta_a$ ,  $\theta_r$ , and  $\theta_i$  are about  $99^\circ$ ,  $32^\circ$  and  $65^\circ$  respectively. It should be emphasised that  $\theta_a$  and  $\theta_r$  form the limits of the hysteresis and are therefore maximum and minimum values.

A possible limiting condition for stable trapping of a gaseous phase within a cavity by a liquid advancing over the surface is that the gas is stable at the mouth and not proud of the surface at the cavity, that is

$$\theta_a \geq 90^\circ + \beta$$

The mean angle  $\theta_{mc}$  on the surface at this critical condition for trapping is then given by eqns. 8(b, c) as

$$\cos \theta_{mc} = s \cos(90^\circ + \beta - \phi)$$

or, rearranging using 8(a),

$$\cos \theta_{mc} = \sqrt{(s^2 - 1)} \cos \beta - \sin \beta. \quad (9)$$

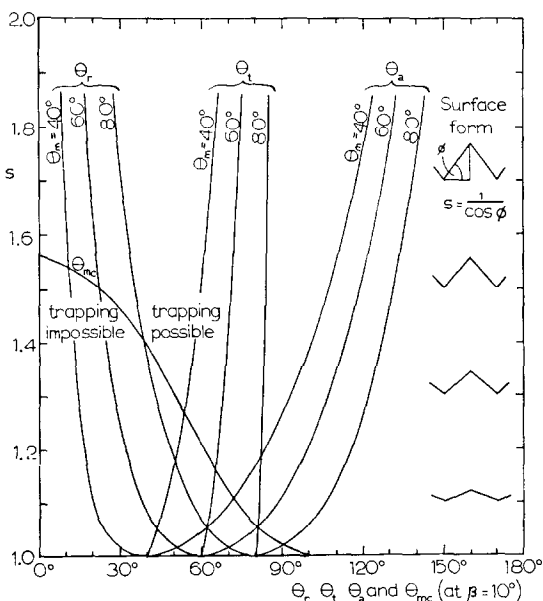


FIG. 6. The effect of micro-roughness on contact angle hysteresis.

The variation of  $\theta_{mc}$  with  $s$  for a cavity with a half-apex angle  $\beta$  of  $10^\circ$  is shown in Fig. 6. Whether or not the gas remains in the cavity once it is trapped depends on the stability of the system as indicated in the previous section. It should be borne in mind, however, that the advancing and retarding angles referred to in this study imply no dynamic effects and any particular stable interface position will remain within the cavity until altered by a surface chemistry change which changes  $\theta_i$ , or (more usually) a change in partial pressure. In the case of a cylindrical cavity,  $\beta = 0$  and

$$\cos \theta_{mc} = \sqrt{(s^2 - 1)}. \quad (10)$$

Experimental confirmation of the general trend of the variation of  $\theta_a$  and  $\theta_r$  with the area ratio or surface roughness is reported by Shepherd and Bartell [10] and Dettre and Johnson [7]. In particular  $\theta_a$  increases and  $\theta_r$  decreases by up to  $30^\circ$  in the initial stages of roughness increase. For rougher surfaces the effects of 'valley-skipping' and surface heterogeneity may alter these functions considerably.

Although the area ratio  $s$  is considered as an indication of surface roughness, it cannot be directly correlated with roughness, as was pointed out by the originator of the concept, Wenzel [11]. Experimental measurements of the area ratio have been made using gaseous adsorption and weighing techniques and are found in a number of surface chemistry textbooks. Machined metal surfaces have typical  $s$  values of 1.1–1.3. For the case of copper, Gregg and Sing [12] have reported a value of 1.18 from adsorption of Argon at 80 K. However, the values depend to some extent upon the nature of the diffusing gas and must be treated with caution. Rhodin [13] reports on the initial stages of oxidation of a very rough copper surface where  $s$  decreases owing to attack of the asperities and filling in of the valleys on the surface.

### 3.3. The effect of surface heterogeneity on the contact angle

Most surfaces contain microscopically varying degrees of contamination leading to differing interfacial energies. Liquid tends to spread preferentially over the areas with low contact angle as shown in Fig. 7. The contamination of metal surfaces is commonly caused by chemical attack (particularly oxidation), adherence of monolayers of organics and gas absorption. Equations (4) and (5) may be combined to give

$$\cos \theta_i = \frac{(\sigma_s - \sigma_{sl}) - \Pi^\circ}{\sigma_{lv}} \quad (11)$$

and contamination is found to affect all the terms in the numerator. In addition  $\Pi^\circ$  varies with the constituents and the pressure of the gaseous phase. Although some progress has been made towards estimating  $\sigma_s$  and measuring  $\Pi^\circ$  from heat of immersion data it is unlikely that this will lead to a reliable means of estimating  $\theta_i$  because the terms have wide ranges and similar magnitudes.

The sensitivity of the contact angle on metals is well

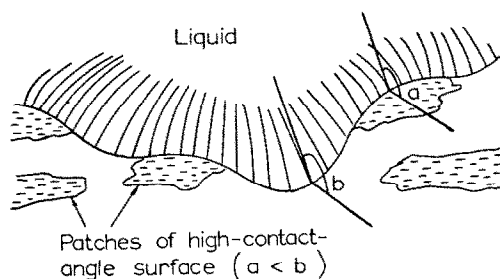


FIG. 7. Liquid on a surface with macroscopic heterogeneity.

illustrated by the case of water on copper. Contact angles have been measured or quoted in the literature with various degrees of precision (see e.g. [14–17, 19]) and range for  $0^\circ$  for pure copper in vacuum to  $87^\circ$  when fully oxidised in air. Nearly all metals very rapidly form a monolayer or more of oxide on the surface when exposed to air, and in the case of copper this layer builds up to around  $0.01 \mu\text{m}$  after a few hours (Rhodin [18]). Ponter *et al.* [16] found that the contact angle decreased from  $76^\circ$  at  $20^\circ\text{C}$  (where most measurements are made) to  $66^\circ$  at  $100^\circ\text{C}$  (where most laboratory boiling experiments are conducted). Under heat transfer conditions when the surface is hotter than the liquid the contact angle was found to decrease by a few degrees.

It is safe to assume that the contact angle will vary considerably with external conditions and from spot to spot on the micro-surface. Some indication of the effect of this variation on the 'non-trapping' area in Fig. 6 is obtained as follows. From Section 3.2 the critical true contact angle  $\theta_{ic}$  below which trapping is impossible may be given as

$$\theta_{ic} = 90^\circ + \beta - \phi. \quad (12)$$

Let  $\Delta\theta_{ic}$  be the increase of true contact angle required (due to the surface contamination and any other effects) to make trapping possible when otherwise impossible.

$$\Delta\theta_{ic} = \theta_{ic} - \theta_t = 90^\circ + \beta - \phi - \theta_t$$

or

$$\Delta\theta_{ic} = (90^\circ + \beta) - \cos^{-1}\left(\frac{1}{s}\right) - \theta_t. \quad (13)$$

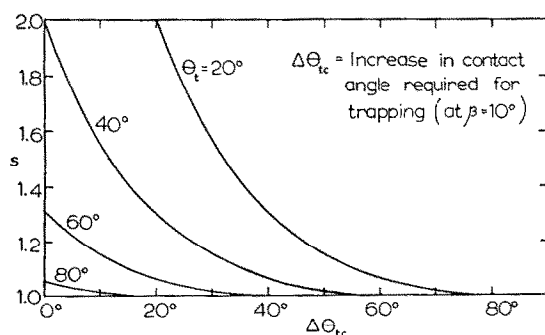


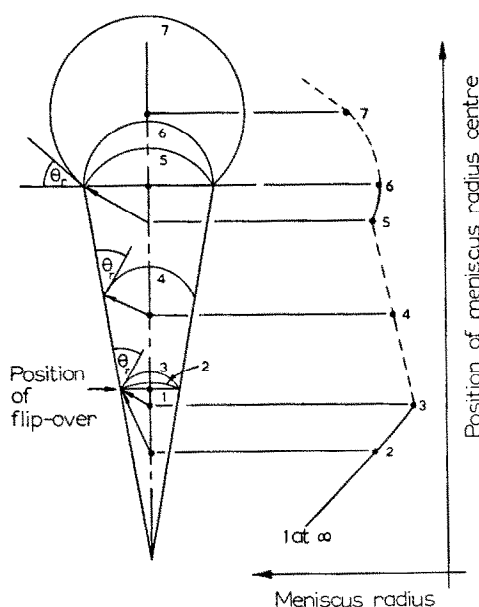
FIG. 8. The effect of a contact angle variation due to heterogeneity on trapping.

This equation is represented graphically for the case of  $\beta = 10^\circ$  in Fig. 8. It is evident that, for water forming a contact angle of around  $60^\circ$  on a typical metal surface of around  $s = 1.2$ , the required contact angle increase is well within the likely scatter of true contact angles on the surface. On the other hand, for angles less than about  $20^\circ$  (as exhibited by many organics) changes of around  $50^\circ$  may be required. As fewer cavity surfaces are likely to deviate by this amount, there will be correspondingly fewer cavities where trapping is possible.

#### 4. THE EFFECT OF CONTACT ANGLE HYSTERESIS ON INCIPIENCE

It was shown earlier that gas and vapour may exist in stable equilibrium in conical cavities with both hydrophilic and hydrophobic surfaces. It now remains to show that the minimum equilibrium radius caused by contact angle hysteresis, rather than the radius at the cavity mouth, forms the main barrier to growth of the gas–vapour mixture.

Figure 9 shows growth from the flip-over position in the cavity. This growth may be caused by gas infusion, evaporation, expansion due to temperature increase or pressure decrease, or a combination of these effects. The retarding angle has been taken as a constant  $40^\circ$ , but similar curves are obtained at other retarding angles (which may range from about  $10$  to  $60^\circ$ , as shown in Fig. 6). Growth from the gas–vapour trapping situations shown in cases (a), (b) and (c) of Fig. 3 are represented in Fig. 9. Case (a) starts at position 2, case (b) at position 3 and case (c) involves passing through flip-over at position 1. Case (d) leads to flip-over and minimum radius at the cavity mouth, but in view of the earlier discussion on hysteresis it is considered unlikely that the interface does not pivot on


 FIG. 9. Meniscus growth following flip-over in a cavity. (Drawn for case of  $\theta_t = 40^\circ$ .)

the side at some point during growth and revert to case (c). The stability criterion, identified as eqn. (2), indicates that the slopes (shown dashed) on the position (or volume) – radius plot in Fig. 9 lead to unstable growth.

It is evident from Fig. 9 that the meniscus radius passes through two minima, at positions 3 and the mouth 6. The radius at position 3 must be less than that at 6 unless the cavity is almost full to the brim with the gas–vapour mixture. It is therefore argued that the radius at position 3 is normally critical and forms the main barrier to incipience. Consequently the cavity mouth radius is normally larger than the equilibrium radius predicted by eqn. (3).

##### 5. CORRELATION WITH EXPERIMENTAL FINDINGS AND DISCUSSION

Although there is a wealth of literature on the effects of surface variables on boiling, surprisingly little of it is directly related to the surface geometry. A common approach [20, 23–25] is to relate both the site density  $n$  and the temperature difference  $\Delta T_{\text{sat}}$  to the effective radius and then to concentrate on the relationship between  $n$  and  $\Delta T_{\text{sat}}$  so that the radius becomes effectively a dummy variable. A model involving the trapping of gas in the cavity in which the contact angle and trapped volume remain constant (see [21]) is now considered rather simplistic in view of the findings of the earlier sections. Both Lorenz *et al.* [21] and Singh *et al.* [22] report that effective radii in artificially produced cavities in boiling and gas diffusion experiments are equal to or less than the measured mouth radius; a result which correlates well with an explanation based on contact angle hysteresis within the cavity.

The extensive experimental studies of [26–29] using natural cavities are directly relevant to this work. Many of the results on contact angle and pressurisation effects are equally explainable in terms of the conventional constant contact angle/re-entrant cavity model and the roughness/flip-over model. For example pressurisation is seen, in the former model, to result in a jump of the liquid in the cavity to a single lower necking or re-entrant point while in the latter model it involves the gradual progression of the advancing liquid down the rough-sided cavity. Retention under moderate pressure release is then possible by the re-entrant geometry in the former case and the roughness–hysteresis effect in the latter case.

However the conventional theory is considered by this author to have a certain disadvantage. In order to allow the trapping of gas and vapor on hydrophilic surfaces it requires the presence of re-entrant cavities or cavities with internal surfaces yielding differing true contact angles. The existence of a large number and size range of re-entrant or necked cavities is considered physically unlikely. The consistency with which every type of machined surface appears to contain boiling sites tends to discredit differing true contact angles as the universal reason for trapping. On the other hand

the roughness/flip-over theory requires only the existence of many positive angled cavities (cones, grooves, scratches, pits) with rough internal surfaces. Examination of machined surfaces under an electron microscope indicates that they are indeed formed almost entirely of this type of ‘cavity’.

In the light of this work the boiling process is seen as follows. There is continuous bubble production at certain sites which, due to their vapour or vapour and gas content, geometry and other factors, have been activated. At any time there are a number of sites which are on the point of incipience and a number on the point of cessation. The slightest change of external or internal conditions (due to thermal interference or turbulence, for example) may be sufficient to change the local site pattern. The precarious equilibrium of the meniscus near the flip-over point necessitates this situation and implies an inherent and time independent change of marginal sites even under steady boiling conditions. The ‘poor reproductibility’ of some individual natural sites [29] and the increasing difference between the accumulated and active sites during boiling [1] are therefore features to be expected.

##### 6. CONCLUSIONS

(1) When the liquid–vapour (or gas) interface in a conical cavity is concave (from the gas side) it is always stable; when convex its stability depends upon the extent of contact angle hysteresis.

(2) Micro-roughness of the cavity walls causes contact angle hysteresis and can lead to a flip-over of the meniscus within the cavity. This flip-over provides a mechanism which allows trapping, storage and subsequent expansion of the gas–vapour mixture under suitable external conditions.

(3) Surface heterogeneity on the microscopic scale also causes contact angle hysteresis and when superimposed on the roughness effects is found to increase the hysteresis range.

(4) Contact angle hysteresis within the cavity (rather than the size of cavity mouth) is shown to form the predominant barrier to incipience. The minimum value of  $R_c$  during incipience is generally less than, (but may be equal to), the cavity mouth radius.

(5) There is a substantial amount of circumstantial experimental evidence that correlates well with the contact angle hysteresis model. The model accounts for incipience without recourse to cavities of special geometry.

*Acknowledgements*—The author is grateful for the facilities provided by the Department of Mechanical Engineering, Heriot-Watt University and the Department of Engineering and Science, University of Iceland. General discussions with colleagues in both Universities and the written comments of Dr. D. B. R. Kenning of Oxford University were of great value in writing this paper.

##### REFERENCES

1. K. Cornwell, *Lett. Heat Mass Transfer* **4**, 63 (1977).
2. S. A. Woon *et al.*, *J. Colloid Interface Sci.* **38**, 605 (1972).

3. J. C. Chen, *J. Heat Transfer* **90**, 303 (1968).
4. P. K. Holland and R. H. S. Winterton, *Int. J. Heat Mass Transfer* **16**, 1453 (1973).
5. R. H. S. Winterton, *J. Phys. D, Appl. Phys.* **10**, 2041 (1977).
6. R. E. Johnson Jr. and R. H. Dettre, *Adv. Chem. Ser.* **43**, 113 (1964).
7. R. H. Dettre and R. E. Johnson Jr., *Adv. Chem. Ser.* **43**, 137 (1964).
8. K. Torikai, H. Shimamune and T. Fujishiro, *4th Int. Heat Transfer Conf., Paris Paper B.2.11* (1974).
9. R. J. Good, *J. Am. Chem. Soc.* **74**, 5041 (1952).
10. J. W. Shepherd and F. E. Bartell, *J. Phys. Chem.* **57**, 458 (1953).
11. R. N. Wenzel, *J. Phys. Colloid. Chem.* **53**, 1466 (1949).
12. S. J. Gregg and K. S. W. Ling, *Adsorption, Surface Area and Porosity*. Academic Press, London (1967).
13. T. N. Rhodin Jr., *J. Am. Chem. Soc.* **72**, 4343 (1950).
14. M. E. Schroder, *J. Phys. Chem.* **78**, 87 (1974).
15. A. B. Ponter et al., *Int. J. Heat Mass Transfer* **10**, 349 (1967).
16. A. B. Ponter et al., *Int. J. Heat Mass Transfer* **10**, 1633 (1967).
17. M. K. Bernett and W. A. Zisman, *J. Colloid Interface Sci.* **28**, 243 (1968).
18. T. N. Rhodin Jr., *J. Am. Chem. Soc.* **72**, 5102 (1950).
19. R. H. Dettre and R. E. Johnson Jr., *J. Phys. Chem.* **69**, 1507 (1965).
20. B. B. Mikic and W. M. Rohsenow, *J. Heat Transfer* **91**, 245 (1969).
21. J. J. Lorenz, B. B. Mikic and W. M. Rohsenow, *Proc. 5th Int. Heat Transfer Conf., Tokyo. Paper B2.1* (1974).
22. A. Singh, B. B. Mikic and W. M. Rohsenow, *J. Heat Transfer* **98**, 410 (1976).
23. M. Shoukri and R. L. Judd, *J. Heat Transfer* **100**, 618 (1978).
24. K. Cornwell, *Proc. 6th Int. Heat Transfer Conf., Toronto. Paper PB-8*. (1978).
25. K. Bier et al., *Proc. 6th Int. Heat Transfer Conf., Toronto. Paper PB-7* (1978).
26. R. I. Eddington, D. B. R. Kenning and A. I. Korneichev, *Int. J. Heat Mass Transfer* **21**, 855 (1978).
27. R. I. Eddington and D. B. R. Kenning, *Proc. 6th Int. Heat Transfer Conf., Toronto. Paper FB1* (1978).
28. R. I. Eddington, Ph.D. thesis, Oxford University (1978).
29. R. I. Eddington and D. B. R. Kenning, *Int. J. Heat Mass Transfer* **22**, 1231 (1979).

#### SUR L'APPARITION DE L'EBULLITION DUE A L'HYSTERESIS D'ANGLE DE CONTACT

**Résumé**—L'apparition de l'ébullition sur une surface métallique est fortement due à l'instabilité des interfaces vapeur-liquide qui existent dans les petites cavités naturelles. Les influences de la rugosité de la surface et de l'angle de contact sur l'équilibre de cet interface sont étudiées et sont établies des expressions reliant la rugosité et l'avance ou le retard de l'angle de contact avec la possibilité de retenue de vapeur.

On présente un modèle d'ébullition basé sur l'hystérésis entre l'avance et le retard de l'angle de contact de l'interface avec la cavité. Cette hystérésis apparaît naturellement du fait de la rugosité et de l'hétérogénéité de la surface à l'échelle microscopique ce qui est le cas des surfaces utilisées pratiquement. Le modèle prédit l'apparition à des rayons plus petits que les rayons de l'ouverture de la cavité et il explique avec succès les observations sur l'ébullition sans postuler l'existence de cavités rentrantes.

#### EINFLUSS DER RANDWINKEL-HYSTERESE AUF DEN SIEDEBEGINN

**Zusammenfassung**—Das Einsetzen des Siedens an einer Metalloberfläche ist weitgehend von der Instabilität der Dampf-Flüssigkeits-Grenzflächen abhängig, welche in sehr kleinen natürlichen Vertiefungen existieren. Es werden die Einflüsse der Oberflächenrauigkeit und des Randwinkels auf das Gleichgewicht dieser Grenzfläche untersucht und Gleichungen entwickelt, welche die Rauigkeit sowie den Ausbreitungs- und Rückzugsrandwinkel mit der Möglichkeit des Dampfeinschlusses in Beziehung bringen. Es wird ein Modell des Siedebeginns angegeben, welches von einer Randwinkelhysterese zwischen Vordringen und Rückzug der Grenzfläche innerhalb der Vertiefung ausgeht. Diese Hysterese ergibt sich zwanglos aufgrund der Rauigkeit und Heterogenität einer Oberfläche in mikroskopisch kleinem Maßstab und kommt deswegen bei normal gefertigten Siedeoberflächen vor. Nach dem Modell erfolgt der Siedebeginn bei kleineren als den Öffnungsradien der Vertiefungen. Es erklärt gut die beobachteten Grundzüge des Siedebeginns, und zwar ohne die Voraussetzung der Existenz höhlenartiger Vertiefungen.

#### ВЛИЯНИЕ ГИСТЕРЕЗИСА КРАЕВОГО УГЛА НА ВОЗНИКНОВЕНИЕ КИПЕНИЯ

**Аннотация** — Возникновение кипения на металлической поверхности в основном обуславливается неустойчивостью поверхностей раздела пар-жидкость в мельчайших естественных углублениях. Исследовано влияние шероховатости поверхности и величины краевого угла на равновесие этой границы раздела и выведены соотношения, описывающие влияние шероховатости и краевых углов на процесс парообразования.

Представлена модель возникновения кипения, основанная на гистерезисе краевых углов границы раздела внутри углубления. Гистерезис вызывается шероховатостью и неоднородностью поверхности раздела на микроскопическом уровне и, таким образом, наблюдается на обычных технических поверхностях кипения. Используя предложенную модель, можно рассчитать возникновение кипения при значениях радиуса, меньших радиуса устья углублений, и успешно объяснить наблюдаемые особенности возникновения кипения, не прибегая к гипотезе повторного заполнения углублений.